NeuroImage **11,** 66–84 (2000)
doi:10.1006/nimg.1999.0516, available online at http://www.idealibrary.com on IDEAL®

Brodmann's Areas 17 and 18 Brought into Stereotaxic Space—Where and How Variable?

Katrin Amunts,*,†,[1] Aleksandar Malikovic,* Hartmut Mohlberg,* Thorsten Schormann,* and Karl Zilles*,†

*C. and O. Vogt Institute for Brain Research, Heinrich Heine University, D-40225, Düsseldorf, Germany and
†Institute of Medicine, Research Center Juelich, D-52425 Juelich, Germany

Received March 29, 1999

Studies on structural–functional associations in the visual system require precise information on the location and variability of Brodmann's areas 17 and 18. Usually, these studies are based on the Talairach atlas, which does not rely on cytoarchitectonic observations, but on comparisons of macroscopic features in the Talairach brain and Brodmann's drawing. In addition, in this atlas are found only the approximate positions of cytoarchitectonic areas and not the exact borders. We have cytoarchitectonically mapped both areas in 10 human brains and marked their borders in corresponding computerized images. Borders were defined on the basis of quantitative cytoarchitecture and multivariate statistics. In addition to borders of areas 17 and 18, subparcellations within both areas were found. The cytoarchitectonically defined areas were 3-D reconstructed and transferred into the stereotaxic space of the standard reference brain. Surface rendering of the brains revealed high individual variability in size and shape of the areas and in the relationship to the free surface and sulci. Ranges and centers of gravity of both areas were calculated in Talairach coordinates. The positions of areas 17 and 18 in the stereotaxic space differed between the hemispheres. Both areas reached significantly more caudal and medial positions on the left than on the right. Probability maps were created in which the degree of overlap in each stereotaxic position was quantified. These maps of areas 17 and 18 are the first of their kind and contain precise stereotaxic information on both interhemispheric and interindividual differences.

INTRODUCTION

Cytoarchitectonic areas 17 and 18 (Brodmann, 1909) constitute the striate and part of the extrastriate cortex in man. Although they belong to the most frequently and intensively studied cortical regions, the analysis of functional organization and their anatomical correlates is a work still in progress. Classical cytoarchitectonic maps are based on a tripartition of the visual cortex and include Brodmann's cytoarchitectonic areas 17, 18, and 19 (Fig. 1). A similar parcellation was suggested by the Russian school (Filimonoff, 1932; Sarkisov *et al.,* 1949). V. Economo and Koskinas presented their own cytoarchitectonic map with a different nomenclature. But, their tripartite principle is comparable with that in Brodmann's map (v.Economo and Koskinas, 1925). Area OC (Area striata) is similar to Brodmann's area 17, their OB (Area parastriata) corresponds to area 18, and OA (Area peristriata)—to Brodmann's area 19. In contrast to Brodmann, they introduced "subregions" which were interpreted as local variations in the laminar pattern within a cytoarchitectonic area. Quantitative criteria were included in support of these delineations.

Functional imaging studies in human and structural analyses in nonhuman primates have contributed to complex maps of the visual cortex (Kaas, 1989, 1995; Fellemann and v.Essen, 1991; Kaas and Krubitzer, 1991; Peterhans and von der Heydt, 1993; Nakamura *et al.,* 1993; Zeki, 1993; Watson *et al.,* 1993; Gulyas and Roland, 1994; Haxby *et al.,* 1994; Shipp *et al.,* 1995; Sereno *et al.,* 1995; Tootell *et al.,* 1995a, 1997; Gattass *et al.,* 1997; Engel *et al.,* 1997; Franca *et al.,* 1997; Zilles and Clarke, 1997). These newer studies have revealed many more areas than described in the classical cytoarchitectonic maps. Experimental data on monkeys have made it possible to draw functionally more relevant anatomical maps and have introduced a different nomenclature (Kaas, 1989, 1993; Fellemann and v.Essen,

[1] To whom correspondence should be addressed at the C. and O. Vogt Institute for Brain Research, Heinrich Heine University, Moorenstrasse 5, D-40225 Düsseldorf, Germany. Fax: +49 211 81-12336. E-mail: katrin@hirn.uni-duesseldorf.de.

1053-8119/00 $35.00

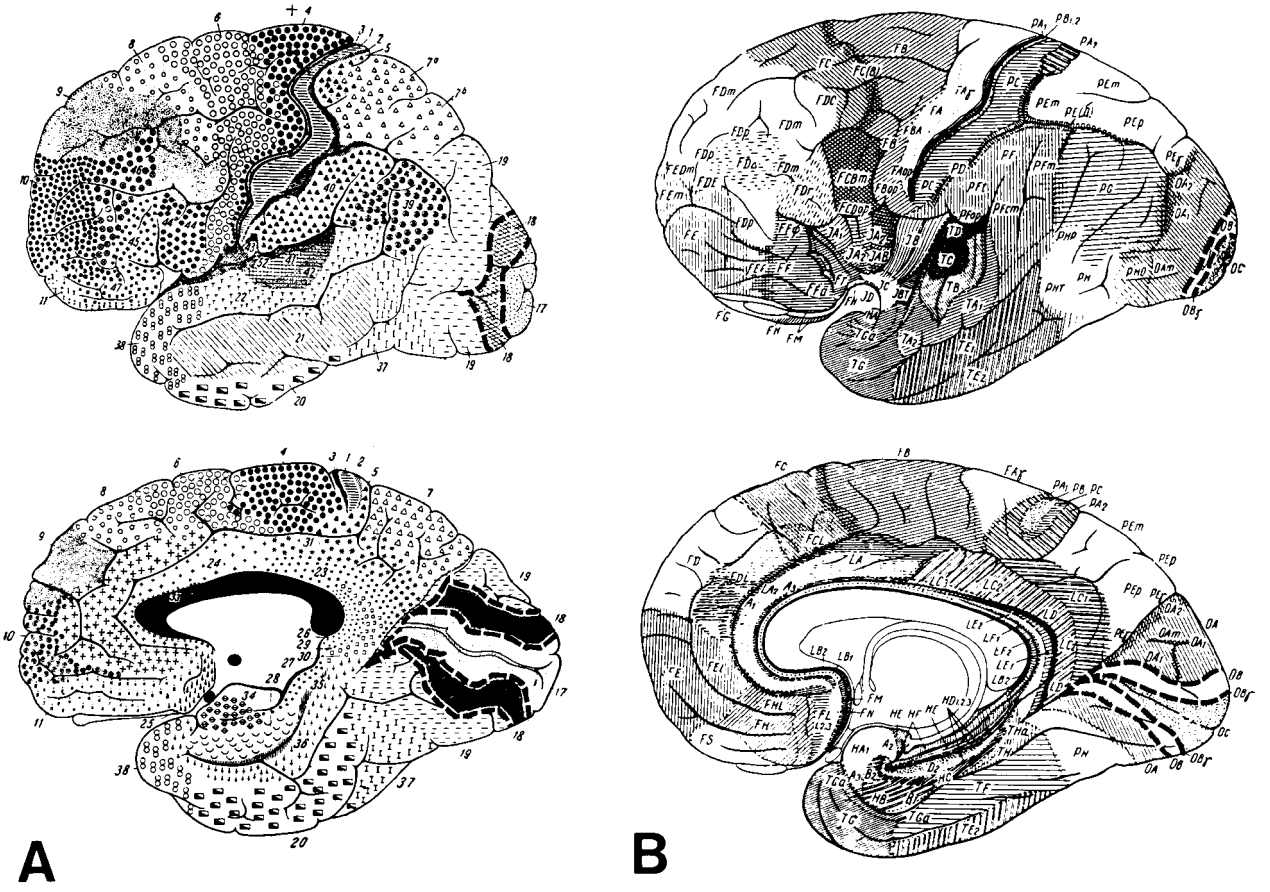

FIG. 1. Cytoarchitectonic maps of Brodmann from 1909 (lateral and medial view; A) and of v.Economo and Koskinas from 1925 (lateral and medial views; B). Brodmann's area 17 corresponds approximately to v. Economo and Koskinas' area OC, Brodmann's area 18—to their OB. Note that areas 17 and 18 occupy a larger portion than OC and OB on the lateral surface and that OB is smaller than area 18 on the mesial surface.

1991; Kaas and Krubitzer, 1991; Zeki, 1993). This nomenclature is widely accepted in imaging studies in man (Lueck *et al.,* 1989; Malach *et al.,* 1995; Shipp *et al.,* 1995; Ungerleider, 1995; Sereno *et al.,* 1995; Tootell *et al.,* 1995a; Tootell and Taylor, 1995b; Aine *et al.,* 1996; Kleinschmidt *et al.,* 1996; Engel *et al.,* 1997; Larsson *et al.,* 1998; Portin *et al.,* 1998). The primary visual area V1 corresponds to area 17. V2 is located next to V1 and may correspond roughly to area 18 (Clarke, 1993). However, we do not know whether cytoarchitectonic areas 17/18 correspond precisely to areas V1/2. For higher visual areas (e.g., V3, V3A, V4, V5) it seems impossible to correlate classical cytoarchitectonic descriptions in man with functional imaging studies (Kaas, 1995). At least area 19 and perhaps area 18 need to be further subdivided. Initial studies have suggested also that human and simian cortical organization may begin to differ in extrastriate cortex at, or beyond, V3A and V4 (DeYoe *et al.,* 1996). Clarification would require an overlay of cytoarchitectonic areas with functionally defined areas in a common reference system. Despite the mismatch between the tripartition of the visual cortex in Brodmann's map and the recent functional and experimental data, the classical maps are still widely used for the anatomical interpretation of imaging data in man.

The maps in Fig. 1 present mainly surface-based information on the location and size of visual areas in relation to gyri and sulci. The idea of whether and/or to what extent architectonic areas are associated with sulci and gyri has been disputed even since Brodmann published his famous map (Brodmann, 1909; Riegele, 1931; Filimonoff, 1932; Sanides, 1963; Rademacher *et al.,* 1993; Amunts *et al.,* 1999a). Therefore, the simple assignment of functional data to particular cytoarchitectonic areas on the basis of anatomical landmarks remains enigmatic. Finally, the individual variability in size, location, and structure of visual cortical areas is not considered either in the maps of Brodmann, v.Economo and Koskinas, and Sarkisov or in the Talairach atlas (Talairach and Tournoux, 1988). This problem can be solved only by applying an anatomical atlas system which is based on a probabilistic approach (Roland and Zilles, 1994; Mazziotta *et al.,* 1995). Such systems are

being successfully applied in other studies on healthy volunteers (Zilles *et al.,* 1995; Geyer *et al.,* 1996; Roland and Zilles, 1996; Gulyas *et al.,* 1997; Larsson *et al.,* 1997; Amunts *et al.,* 1998; Larsson *et al.,* 1997, 1998) as well as in clinical research (Thompson *et al.,* 1998).

The aim of this study was

(a) to create cytoarchitectonic maps of areas 17 and 18 from serial histological sections of 10 human brains using a statistical approach for defining borders,

(b) to transfer these maps into the three-dimensional stereotaxic space of the standard reference brain,

(c) to define the spatial extent and location of each area in the standard system, and

(d) to analyze intersubject variability.

MATERIAL AND METHODS

Ten human brains were examined: five male and five female brains ranging in age from 37 to 85 years (Table 1). The brains were obtained from body donor programs. The autopsy was performed within 8 to 24 h after death. Brain 3 came from a subject with transitory motor disturbances, all the other subjects had no medical history of neurological or psychiatric diseases. Handedness of the subjects was unknown. Considering an incidence of right-handedness in approximately 90% of the population (Gilbert and Wysocki, 1992), most of our cases will have been right-handed.

After the brains were removed from the skull they were fixed in 4% formalin (cases 2–8) or in Bodian, a mixture of formalin, glacial acetic acid, and ethanol (remaining cases). Brains were hung up by their vertebral arteries in the fixative in a freely movable manner, which enabled a minimum of distortions in brain shape. The meninges were removed after several months of fixation. MR imaging was carried out as previously described and validated (Roland and Zilles, 1994; Zilles *et al.,* 1995; Amunts *et al.,* 1996; Geyer *et al.,* 1996). Imaging was performed with a Siemens 1.5-T magnet (Erlangen, Germany) with a T_1-weighted 3-D FLASH sequence covering the entire brain (flip angle 40°, repetition time TR = 40 ms, echo time TE = 5 ms for each image). Each volume consisted of 128 sagittal sections. The spatial resolution was 1 × 1 × 1.17 mm (Steinmetz *et al.,* 1990). The image space was divided into voxels in the form of rectangular parallepipeds of uniform size, each with a resolution of 8 bits corresponding to 256 gray values. The image sequences were 3-D reconstructed.

TABLE 1

List of Brains

Case	Age (years)	Gender	Cause of death	Fresh weight (g)
1	79	F	Carcinoma of the bladder	1350
2	55	M	Rectal carcinoma	1270
3	68	M	Vascular disease	1360
4	75	M	Acute glomerulonephritis	1349
5	59	F	Cardiorespiratory insufficiency	1142
6	54	M	Cardiac infarction	1757
7	37	M	Cardiac arrest	1437
8	72	F	Renal arrest	1216
9	79	F	Cardiorespiratory insufficiency	1110
10	85	F	Mesenteric infarction	1046

The brains were then embedded in paraffin and sectioned in the coronal plane through both hemispheres. From brains 1–4, the cerebellum and the brain stem were removed above the mesencephalon prior to embedding. The others were processed *in toto.* From each brain 6000–7500 sections (20 μm) were acquired. Each 15th section was mounted on glass slides and silver stained for perikarya (Merker, 1983). In brains 1 and 2, in addition to the sections stained for cell bodies, neighboring sections were stained for myelin (Gallyas, 1979). Each 60th section of the entire series was used for analysis. Images of the histological sections were digitized and 3-D reconstructed. The 3-D reconstructions were matched to the MR sequences of the brains, which were obtained prior to embedding and sectioning. This enabled us to exclude inevitable distortions caused by histological techniques such as by sectioning and by mounting on glasses. Matching was performed by using both linear and nonlinear fluid transformations (Schormann *et al.,* 1993, 1995; Schormann and Zilles, 1997, 1998, 1999). Nonlinear fluid transformations were applied for matching the 3-D reconstructions to the MR sequences of the brains. Finally, brains were warped to the standard format of the reference brain (Roland and Zilles, 1994, 1996, 1998) using affine transformations, i.e., only shifting, scaling, and rotating. The orientation of the brains was in the plane determined by the anterior–posterior commissures, i.e., the AC-PC plane (Talairach and Tournoux, 1988). Images of all brains were divided into sequences for the left and the right hemispheres. From images of brains 5–10, the cerebellum was removed in order to expose the mesial surface. Surface rendering of the image sequences was performed using the software AVS (Uniras).

Cytoarchitectonic analysis was performed by measuring the gray level index (GLI) in regions of interest (ROIs). The GLI (Zilles *et al.,* 1986; Schleicher and Zilles, 1990) is a measure of the volume fraction of somata per volume unit brain tissue. It is highly correlated with cell density (Wree *et al.,* 1982). The ROIs covered those parts of the cortex in which a cytoarchitectonic border was microscopically apparent. ROI size varied in dependence on cortical thickness and sulcal properties up to approximately 1.5–2 cm^2. Measurements were performed using an image analyzer (KS400; Zeiss) connected to a microscope with a motor stage for automated scanning and focussing. Digitized,

high-resolution GLI images of the ROIs were obtained and printed. The GLI of each pixel in these images represents the volume fraction occupied by cell bodies in a square measuring field of 32 × 32 μm (Figs. 2–4).

Laminar changes in cortical cell density were registered as GLI profiles from the border between layers I and II to the border between cortex and white matter. The profiles were oriented along trajectories running parallel to the orientation of cell columns, i.e., perpendicular to the cortical surface. Profiles covered the cortex in the ROIs at equidistant intervals of approximately 128 μm. The positions of profiles were numbered consecutively from 1 to n, where n was the number of profiles per ROI. The laminar pattern of each GLI profile was characterized by a set of 10 features (=feature vector) based on central moments (Pearson, 1936; Dixon *et al.,* 1988). The features included the mean GLI value, the center of gravity in axis of the cortical depth, the standard deviation, the skewness, the kurtosis, and the analogous parameters for the first derivative of each profile (Amunts *et al.,* 1997; Schleicher *et al.,* 1999).

The observer-independent definition of borders (Schleicher *et al.,* 1998, 1999) is based on the assumption that the laminar pattern of the GLI is similar within a cytoarchitectonic area, but changes abruptly at the border between two areas. Using feature vectors, we performed a multivariate statistical analysis between two neighboring blocks of profiles in order to detect differences between the blocks in the laminar pattern. A non-Euclidean distance function, the Mahalanobis distance function, has been applied for quantifying laminar differences. The blocks were shifted simultaneously in steps of one profile over the entire cortical region of interest. The distance between neighboring profiles and, thus, the step width was approximately 128 μm. The Mahalanobis distance D^2 was calculated continuously for each position of the blocks in order to quantify the degree of differences in the laminar patterns (Figs. 2–4). Previous studies have shown that the block size, i.e., the width of a block, does not influence the appearance and the position of detected borders in a large interval (Fig. 3). A subsequent Hotellings' t^2 test was applied for testing the significance of D^2 ($\alpha = 0.05$ for all tests). The higher the D^2 value between two blocks of profiles, the greater the differences in the laminar patterns, and vice versa, the lower the D^2, the more similar the profiles. Borders between cytoarchitectonic areas were defined at positions at which differences in the laminar patterns were significant (Schleicher *et al.,* 1999).

The interpretation of cortical entities was performed mainly on the basis of v.Economo and Koskinas' map (1925). Their descriptions were more detailed than those of Brodmann (1903, 1909) and were based on several brains. The area OC of v.Economo and Koskinas corresponds to Brodmann's and our area 17 as well as to the striate area of Elliot Smith (1907). Their OB corresponds to Brodmann's and our area 18 and to the parastriate area of Elliot Smith. As we mentioned in the Introduction, the concept of area 19 in man as proposed by Brodmann (1909) clearly needs to be revised. But, at present, there are no exhaustive anatomical maps of the human visual cortex as there are for the monkey (Fellemann and v.Essen, 1991). For practical reasons therefore, we use for the region which surrounds area 18 the term "area 19," knowing that it encompasses several higher visual areas.

The positions of areas 17 and 18 in the histological sections were transferred onto their computerized images. Images of both areas were 3-D reconstructed and transferred into the corresponding images of the whole brains (Figs. 5 and 6). Surface rendering of the brains was performed using the software AVS (Uniras, Germany). Areas 17 and 18 were aligned to the standard format of the reference brain using the same affine transformations as were applied for the whole brains (see above). The spatial resolution of the images in standard brain format is 1 × 1 × 1 mm. In a final step, areas 17 and 18 were overlapped in the 3-D stereotaxic space of the reference brain. The volumes of areas 17 and 18 in the standard reference system were calculated and compared between hemispheres and sexes (two-way ANOVA with repeated measurements design; $P < 0.05$). Mean volumes of both cytoarchitectonic areas were calculated by averaging individual volumes. Since the mean volumes were calculated in the standard space, they are normalized, but the application of only linear tools for the alignment of the areas maintained their individuality in volume and shape.

The extent of each area in the coronal, sagittal, and horizontal axis was calculated in Talairach coordinates (Table 2) and averaged over the entire sample. The coordinates of both areas were compared with those of the Talairach/Tournoux atlas (Talairach and Tournoux, 1988). Centers of gravity were compared for both areas and hemispheres using a two-way ANOVA with repeated-measurements design and subsequent Bonferroni t test ($P < 0.01$). The number of overlapping brains per voxel was calculated and color coded. The representations of all areas 17 and 18 in the format of the standard reference brain are called "probability maps" or "population maps" (Roland and Zilles, 1994, 1996). Such maps are shown for areas 17 and 18 in Fig. 7. The 50% volumes were defined as all those voxels of the probability map which belong to 5 or more of the 10 brains.

RESULTS

The borders between areas 17 and 18, and between 18 and neighboring higher visual areas, were defined in

all 10 brains quantitatively. We found significant differences between the shapes of cell density profiles in areas 17 and 18 using multivariate statistical analysis. The distance function showed maximal values if the profiles were located at either side of an areal border. The laminar distribution pattern of cell bodies, i.e., the feature vectors, differed significantly ($P < 0.05$) between areas 17 and 18, as well as between area 18 and the higher visual areas in all samples (Figs. 2–4). In only approximately 2% of the cases did a significant "border," detected by the automated procedure, need to be rejected. Abrupt changes in the orientation of the cell columns and/or histological artifacts which alter the laminar pattern had been detected. They were always easily recognizable and showed up clearly localizable in the distance function curve.

Although the positions of borders of areas 17 and 18 were mapped by applying a statistical approach for the definition of borders, the identification of the area between two borders was based on criteria which have been described in the classical cytoarchitectonic studies (Brodmann, 1903; v.Economo and Koskinas, 1925; Filimonoff, 1932). Area 17 contained a prominent layer IV which could be further subdivided into three sublayers. Layers III and V were characterized by small cells. Layer V appeared light and was easily distinguished from the dark layer VI. The layering of this area was very distinct. The area was limited to the ventral limb of the calcarine sulcus only in the most rostral sections. The border of area 17 was always easy to identify: layer IV became considerably thinner when moving from area 17 to area 18 and its subdivision into three sublayers stopped abruptly (Fig. 2).

In area 18, layer II bordered indistinctly upon the upper part of layer III, which was cell dense. The size of the pyramidal cells of layer III was increased from the upper to the lower levels. Large cells in deep layer III were found immediately after the border from 17 to 18 was crossed. Single cells of similar size were present in layer V. The contrast in density between layers V and VI was not as high as in area 17. Layer IV was thinner than in area 17, but thicker than in the higher visual areas. The clarity of the columnar arrangement in the areas increased from 17 over 18 to the higher visual areas. This feature was of special importance for the border of area 18 to higher visual areas.

Several cytoarchitectonic changes could be found at the border of areas 17/18 which did not coincide with the one in layer IV. For example, the orientation of cell columns toward the pial surface was lost in a small zone of area 17 which was located immediately in front of the border to area 18. Layers III and IV were especially involved. In addition, layer VI became as dense as in area 18 before the abrupt change in layer IV occurred, i.e., in the last portion of area 17. A small zone with a very light layer V was often found at the beginning of area 18. The cells in this zone were less densely packed than in the remaining part of area 18.

We compared the cytoarchitectonic transition zone between areas 17 and 18 with its myeloarchitecture in two brains. The transition was characterized by two regions (Lungwitz, 1937; Sanides and Vitzhum, 1965a,b). Subarea Gb (border tuft, i.e., "Grenzbüschel") had a distinct bundle of myelinated radial fibers located at the beginning of area 18. When moving in the direction of the 17/18 border, the myeloarchitecture as well as the cytoarchitecture underwent gradual changes. This part of area 17 was called "fringe area," i.e. "Randsaum" (Rs) (Fig. 2B).

In correspondence to this heterogeneity of areas 17 and 18 in myeloarchitecture (e.g., fringe area, border tuft), we found further significant borders within each area in the sections stained for cell bodies. They subdivided 17 and 18 into two or more parts. Each of them extended approximately 3–8 mm along the cortical surface (for examples, see Figs. 2 and 3). These internal borders were not caused by technical artifacts and could be identified on adjacent sections. In some cases, they were found at the transition between the crown and the wall of a gyrus (e.g., border within area 18 at positions 60 and 74 in Figs. 2 and 3). Others did not coincide with changes in gyral geometry (e.g., border at position 49 in Figs. 2 and 3). Some of these borders corresponded to those described by Sanides and Vitzhum, e.g., the border at position 16 marked subarea Rs and that at position 26 marked subarea Gb (Sanides and Vitzhum, 1965a,b).

In area 18, zones with striking pyramidal cells sometimes alternated with zones with relatively smaller cells in layer III (Fig. 2). The laminar pattern in the other layers remained unchanged. In Fig. 2 as in many other sections, the subparcellations were related to changes in the sizes of pyramidal cells in deep layer III: In the region between positions 49 and 60, these cells were especially prominent, whereas between positions 60 and 80 they were small. In some sections, a zone with especially large pyramidal cells, i.e., giant cells, was observed close to the border of areas 17 and 18. The laminar pattern of this zone corresponded to that of OBγ as described by v.Economo and Koskinas (1925). The border tuft (Gb) was located within this area. The border of OBγ within area 18 was sometimes difficult to recognize since the size of the pyramidal cells decreased gradually. OBγ was not always present: in other sections, the pyramidal cells were not striking and did not allow identification of the OBγ either by visual inspection or quantitatively (e.g., Fig. 2). If present in the histological section, the border of OBγ was defined quantitatively (v.Economo and Koskinas, 1925).

Taken together, the above cytoarchitectonic features allowed the identification of areas 17 and 18 and their distinction from neighboring areas. However, the complexity of cytoarchitectonic changes at the transition of two cortical areas makes it necessary, even in such a "simple" case as between areas 17 and 18, to analyze these borders quantitatively.

The individual brains and their cytoarchitectonic areas were transformed into the standard format of the reference brain (Figs. 5 and 6). This transformation allowed us to compare areal positions, extents, and sizes regardless of differences in absolute brain size. Area 17 was always located ventrally and dorsally at the bottom of the calcarine sulcus. Only at the most rostral sections was area 17 located on the ventral limb of the calcarine sulcus and not on the dorsal limb. In these sections as in all other coronal sections, area 17 was flanked by area 18 in the dorsal and ventral directions. The calcarine sulcus differed in shape and the number of its segments between the hemispheres (compare, e.g., case 10 with remaining cases in Fig. 6). The location of the border between areas 17 and 18, and between 18 and higher visual areas, was variable with respect to the free surface of the cuneus (compare, e.g., case 10, right side, with 6, right side, and 4, left side). Both areas were limited dorsorostrally by the parietooccipital sulcus. On the most rostral sections, areas 17 and 18 did not reach the free surface of the parietal lobe and were located in the ventrocaudal bank of the parietooccipital sulcus. The most caudal portion of the occipital lobe was occupied by area 17 to a different degree (Fig. 5). Thus, brains differed significantly with respect to shape, size, and location as projected on the surface of the brain.

The mean volumes of areas 17 and 18 did not differ significantly between the hemispheres. For area 17, six brains had a larger volume on the left than on the right side. In area 18, five brains were larger on the left than on the right (for both areas $P > 0.05$). These differences were independent of gender. The volumes of left and right areas 17 were significantly larger than the volumes of areas 18 ($P < 0.05$). The volume of area 17 (both sides together) was 23.3 cm^3 (SEM 1.1), that for area 18 (both sides together) was 19.5 cm^3 (SEM 1.2). These differences were independent of the side ($P > 0.05$).

Table 2 gives an overview of the ranges of both areas and of the centers of gravity in the stereotaxic space (Talairach and Tournoux, 1988). Ranges and centers of gravity were averaged over the whole sample. The locations of centers of gravity for both areas differed significantly between the hemispheres. The centers on the right were located more laterally than those on the left (two-way ANOVA: $P < 0.01$, $df = 9$, $F = 42.8$). The centers of gravity on the left were located more caudally than those on the right (two-way ANOVA: $P < 0.01$, $df = 9$, $F = 28.4$). The more caudal position of left areas 17 and 18 was found in all 10 cases. It is interesting to note that both occipital poles tended to point to the right (Table 2, fourth column). Parts of left areas 17 and 18 were located to the right of the medial plane (i.e., the AC-PC line). In brains 4, 5, 8, and 10 this was especially apparent (Fig. 5).

Comparing areas 17 and 18, it was found that the centers of gravity of area 18 were located more laterally than those of area 17 (two-way ANOVA: $P < 0.01$, $df = 9$, $F = 89.3$). Area 17 extends to a more caudal position than area 18 (two-way ANOVA: $P < 0.01$, $df = 9$, $F = 29.3$). Whereas the most ventral positions of areas 17 and 18 were similar for left and right hemispheres, the most dorsal positions of area 18 are higher than those of area 17 (Table 2, 9th and 10th columns). The centers of gravity in the z direction were similar for both hemispheres.

The corresponding coordinates of the stereotaxic atlas of Talairach and Tournoux (1988) are compared in Table 3. The coordinates of Talairach/Tournoux fall within the ranges of our sample but tend to underestimate the extent of both areas. This is especially true for the sagittal extent of areas 17 and 18 on the right.

Probability maps were created for further analysis of spatial variability. They contain information on the probability of a given area being present at a given position, i.e., in an individual voxel of the reference system of the standard brain. Each voxel therefore represents the number of brains that overlap at that point and was color-coded to represent that number. Probability maps are shown in the coronal, sagittal, and horizontal planes (Fig. 7). Area 17 of all brains was located mainly in the depth of the calcarine sulcus. In the most occipital sections, it extended farther onto the free surface. Area 17 was least variable in the bottom of the sulcus. The rostral border of the probability map of area 17 approached the corpus callosum of the standard brain. The probability maps of area 18 surrounded those of area 17 dorsally and ventrally (notice the two foci of high probability above and below the calcarine sulcus in the sagittal and coronal sections).

Variability between the 10 brains was further quantified. The volume of each area was calculated as it relates to the number of overlapping brains (Fig. 8). The bar chart shows large volumes for small numbers of overlapping brains and small volumes for regions of high overlap. Area 17 had a higher degree of overlap than area 18. The decrease in volume relative to the number of brains was less steep in area 17 than in 18. Comparing the 50% volumes with the mean volumes further quantified this finding. Whereas the 50% volume of area 17 occupied about 72% of the mean volume of the area, the 50% volume of area 18 occupied only 40% (Fig. 9).

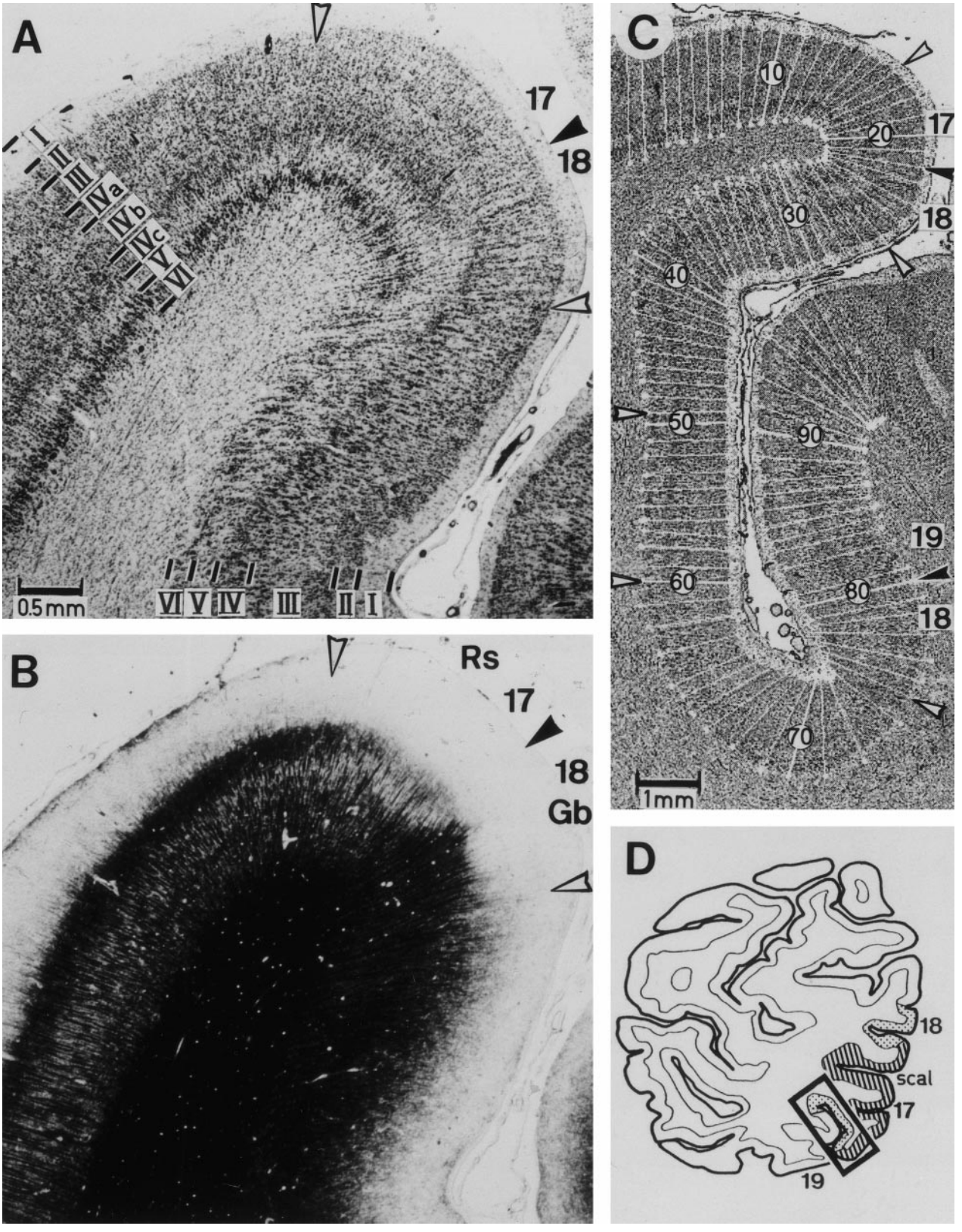

FIG. 2. Cytoarchitecture and myeloarchitecture at the transition between areas 17 and 18 in brain 1 (section 901, left hemisphere, ventral border of area 17). (A) The cytoarchitecture changes abruptly at the border between both areas—especially prominent are changes in layer IV, which becomes thinner and less differentiated in area 18 than in area 17. (B) The myeloarchitecture on the neighboring section shows the border at the same position. Near the border between areas 17 and 18, but within area 17, both the myeloarchitecture and the cytoarchitecture change gradually (= "fringe area" or "Randsaum"). In addition, subarea Gb (border tuft, i.e., "Grenzbüschel") can be delineated. These subdivision were described by Sanides and Vitzhum (1965a,b). The border tuft is located within v.Economo's and Koskinas' area OBγ

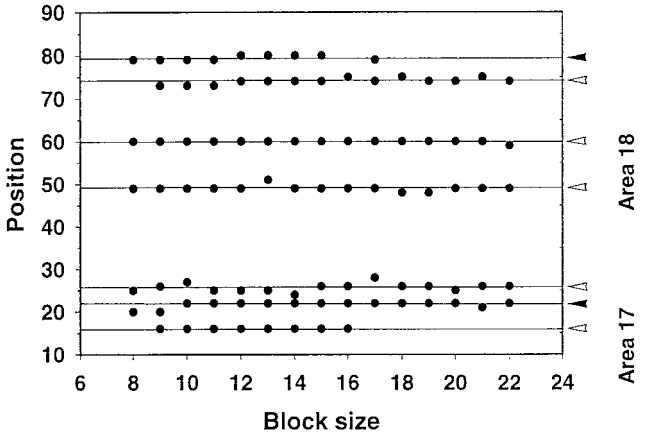

FIG. 3. Positions of significant maxima of the Mahalanobis distance function D^2 versus block size (in pixel) of section 901, case 1 (corresponding to Fig. 2). The positions are shown in Fig. 2C. Black arrowheads mark the borders of area 18 at positions 22 and 80. White arrowheads indicate borders within area 17 (at position 16) and within area 18 (at positions 26, 49, 60, and 74), i.e., internal borders. Each D^2 value was calculated for the distance between two neighboring blocks of profiles with a certain number of profiles in each. The number of profiles defines the block size and ranges from 8 to 22. Comparing the positions of internal borders with the cytoarchitecture, it seems that the border at position 16 marks the beginning of the border tuft. The border at position 26 in Fig. 2C seems to mark the ending of the fringe area. The borders at positions 49 and 60 do not represent a documented cytoarchitectonic border, but they occur regularly and are regardless of block size and cannot be interpreted as a result of technical artifacts.

DISCUSSION

The cytoarchitecture of the visual cortex has been the subject of intensive research for many decades (Brodmann, 1903, 1909; v.Economo and Koskinas, 1925; Filimonoff, 1932; Zilles *et al.,* 1986; Leuba and Garey, 1989; Zilles and Schleicher, 1993). The same applies to the myeloarchitecture (Vogt and Vogt, 1919; Flechsig, 1927; Lungwitz, 1937; Sanides and Vitzhum, 1965a,b; Zilles and Schleicher, 1993) and the connectivity of these areas (Burkhalter and Bernardo, 1989; Clarke and Miklossy, 1990; Clarke, 1993; v.Essen *et al.,* 1993; Stepniewska and Kaas, 1996). Pigmentoarchitecture (Braak, 1977), cytochrome oxidase (Wong-Riley *et al.,* 1993; Clarke, 1994), and receptor architecture (Zilles and Schleicher, 1993; Zilles and Clarke, 1997) have also been examined. For an overview see Zilles and Clarke (1997). Functional imaging studies have further enhanced our knowledge about the organization of the visual cortex but also required more precise and reliable anatomical maps for the topographical interpretation of activation clusters. The decision of whether an activation cluster is within or outside an architectonic region can be solved only if the border of this region is determined. It is well known that area 17 is located in the depth of the calcarine sulcus, but the positions of its borders on the mesial surfaces of the hemispheres and on the occipital poles vary from case to case (Filimonoff, 1932; Stensaas *et al.,* 1974). For area 18 and many other cortical areas, no reliable landmarks indicate the precise or approximate positions of borders.

The automatic detection of the border between areas 17 and 18 was a good proof of the reliability of the automated approach for border definition since it is one of only a few cortical borders which can readily be recognized in histological sections (Schleicher *et al.,* 1999). A comparably obvious border separates the primary motor and the somatosensory cortex, i.e., Brodmann's areas 4 and 3. A distinguishing feature of area 17 is the structure of layer IV which becomes abruptly altered at the border to 18. The change in layer IV was therefore chosen for defining the border between areas 17 and 18 (v.Economo and Koskinas, 1925). In this sense, the border between both areas is clear.

This is, however, not the only architectonic change at the transition between the two areas (Filimonoff, 1932). Two myeloarchitectonic subareas (Rs, Gb) have been identified; one belongs to area 17, the other to area 18 (Lungwitz, 1937; Sanides and Vitzhum, 1965a,b). These subareas appeared in our myelin-stained sections and were also detected in the sections stained for cell bodies. In the latter, they were identified as significant peaks in the distance function. Quantitative analysis of the cytoarchitecture revealed further subdivisions within areas 17 and 18. Subtle changes in the laminar patterns were seen in the microscope, but they were difficult to follow in larger series. Their description was further complicated by the geometry of the gyri. Occipital gyri are relatively small and architectonic borders are often located in curved regions, not at the plane surface of the brain or of a gyrus (e.g., Fig. 2). In our sample, at least in some sections, subparcellations of area 18 were associated with the presence or absence of large pyramidal cells in deep layer III. One of the first studies to mention such inhomogeneities within area 18 (OB) was that of v.Economo and Koskinas (1925)

(v.Economo and Koskinas, 1925). This part of area OB, which is characterized by especially large pyramidal cells in layer III, is, however, in this, as in some other sections, not clearly visible. (C) The digitized image with a cortical region containing larger parts of areas 17 and 18. The gray value of each pixel in this image indicates the volume fraction of cell bodies, which is a good estimate of cell packing density: a high GLI is represented by a dark pixel, a low GLI by a brighter pixel. The cortex is covered with vertical lines ("traverses") running from the border between layers I and II to the cortex/white matter border. Along each line, a GLI profile was measured. The positions of the profiles were numbered (in this case, from 1 to 96) with equidistant intervals of approximately 128 μm. (D) Location of the GLI image (C) in the hemisphere. *scal,* calcarine sulcus. Roman numerals indicate different cortical layers.

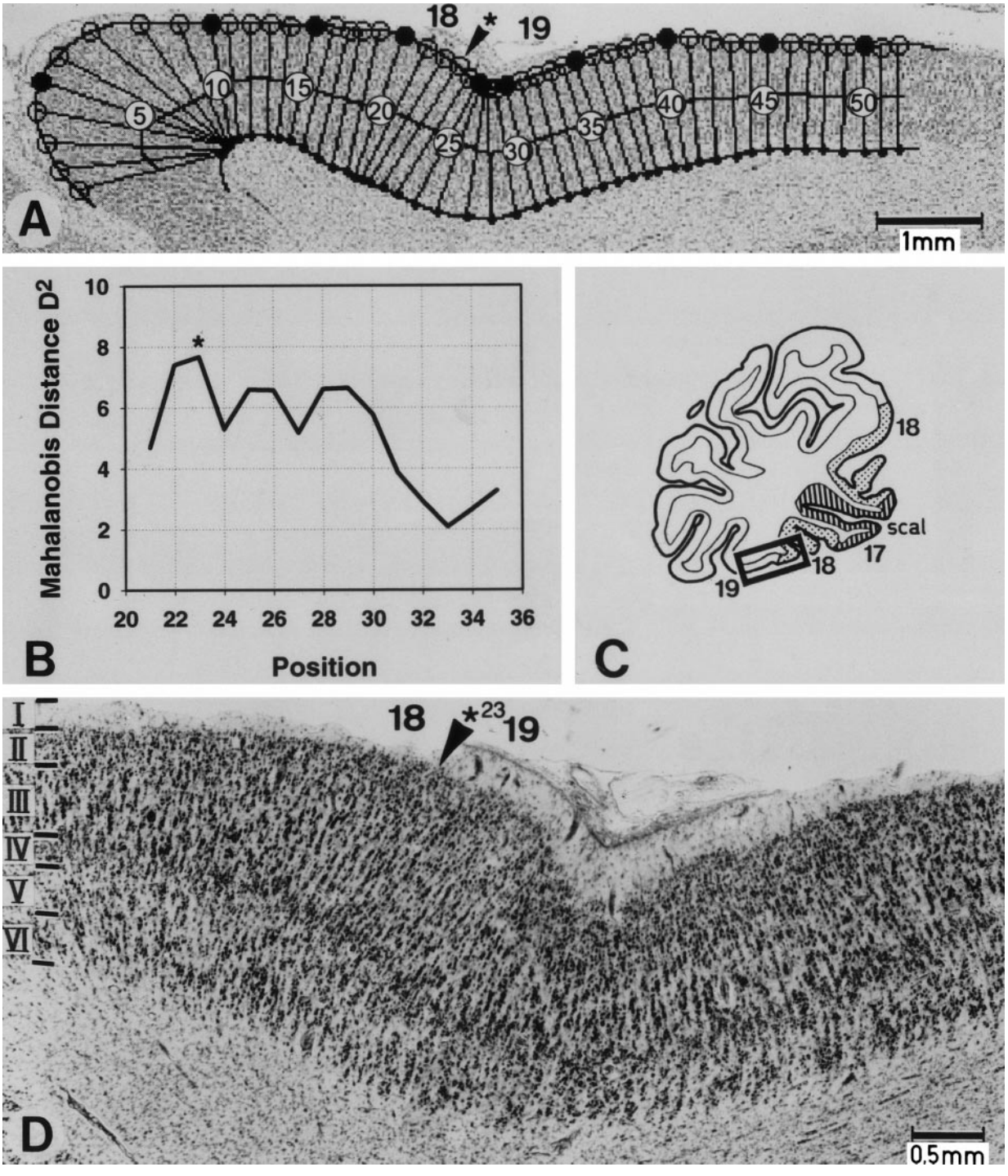

FIG. 4. Borders between areas 17 and 18 in brain 5 in two neighboring sections: sections 841 (A–D) and 901 (E–H). The distance between the sections is 1.2 mm. (A, E) GLI image of the region of interest. The positions of profiles are numbered from 1 to 52 (A) and from 1 to 56 (E). (B, F) The distance function D^2 depending on the position of the profile. Significant peaks of D^2 were found at positions 23 (B) and 24 (F). The significant peaks of D^2 exactly match the ventral border of area 18 to area 19 (black arrowheads). The positions of the borders coincide in the two neighboring sections. (C, G) Location of the GLI image at the hemisphere. (D, H) Micrographs of a coronal, silver-stained section with marked border between areas 17 and 18 corresponding to the results from the analysis of D^2. Roman numerals indicate different cortical layers.

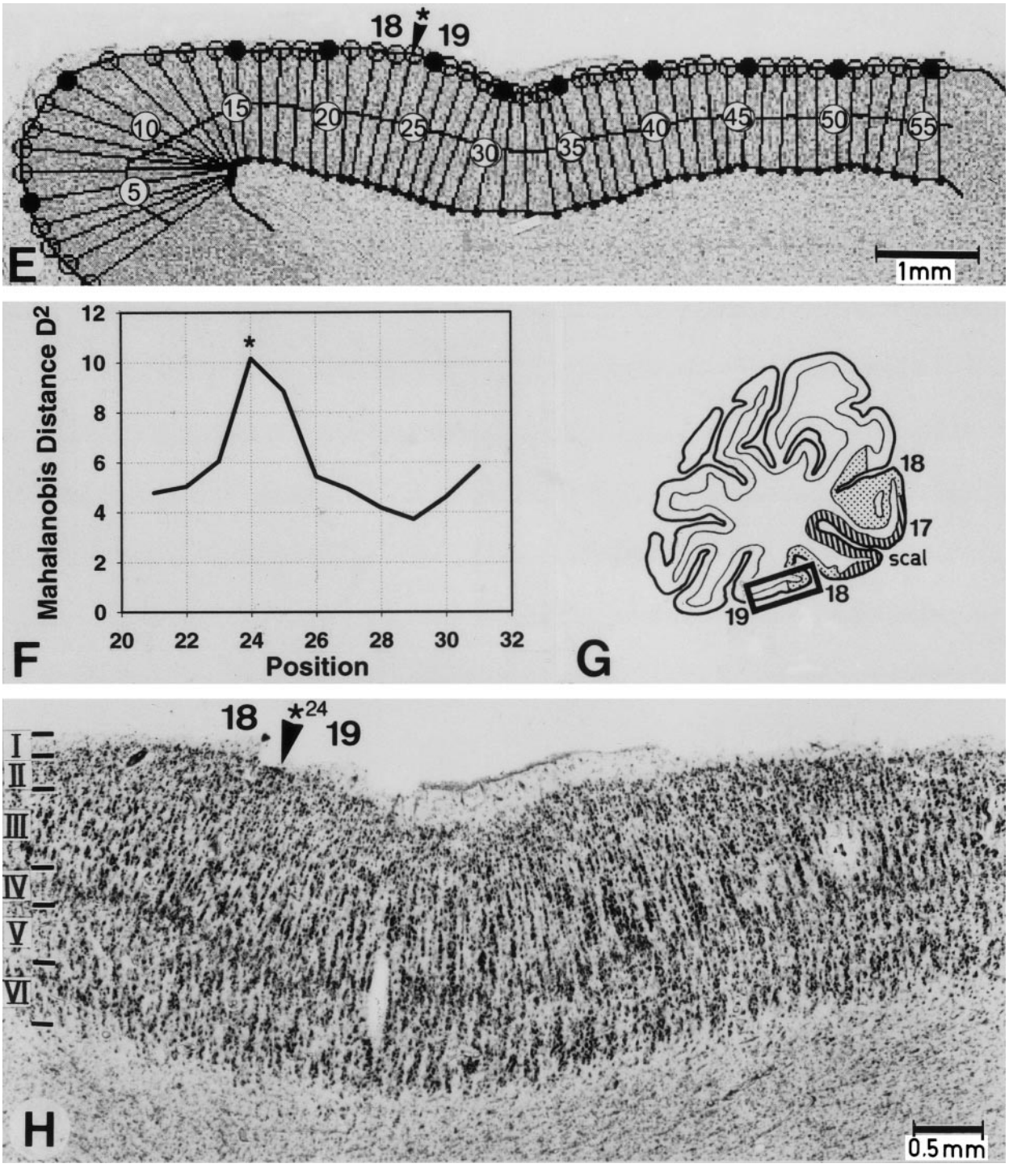

FIG. 4—*Continued*

who described subarea OBγ. We found this subarea in several sections and verified it quantitatively (see also Schleicher *et al.,* 1999). Our findings are in good agreement with earlier studies which reported that this subarea is not present in all sections (Vogt, 1929; Filimonoff, 1932). V.Economo and Koskinas noticed scattered conglomerates of granule cell (OBΩ), but their description did not allow us to identify these subareas reliably.

A better understanding of cytoarchitectonic inhomogeneities in human areas 17 and 18 may come from studies analyzing the connectivity of the visual cortex

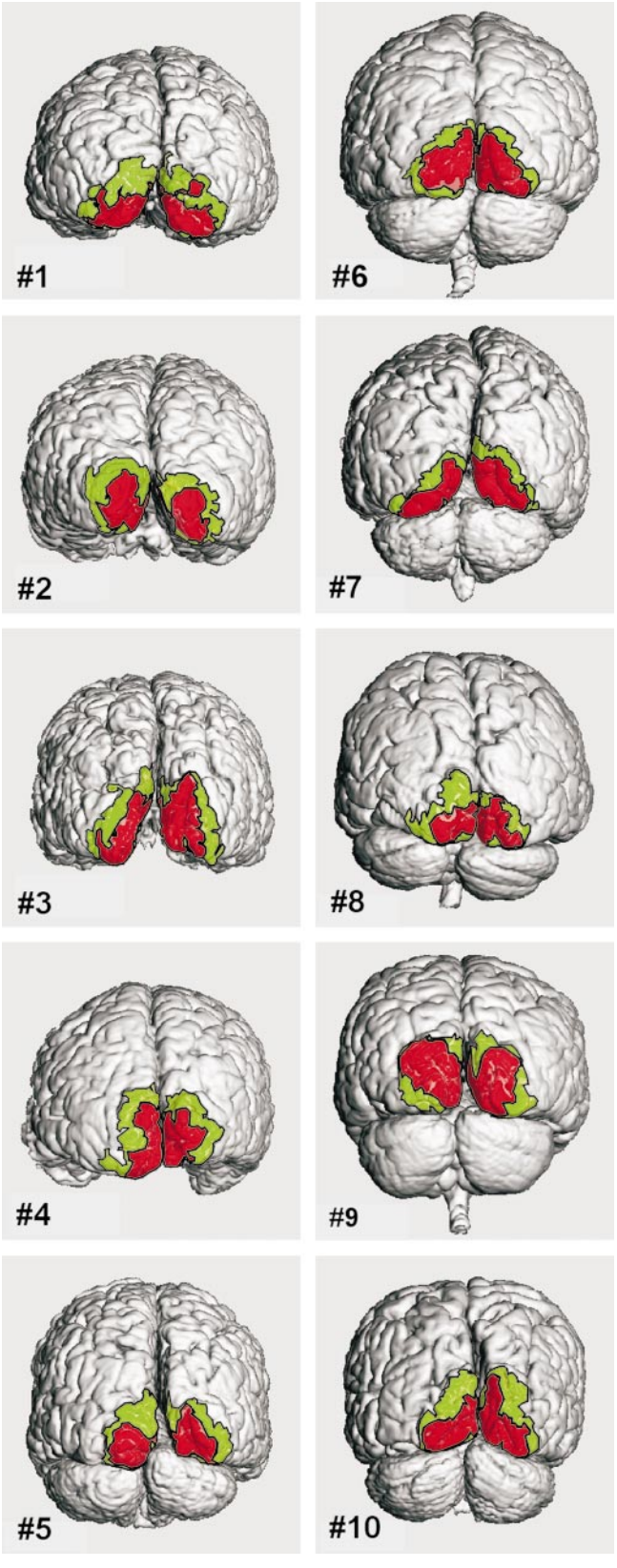

and the pattern of cytochrome oxidase both in human and in the macaque. "Callosal-rich" and "callosal-poor" regions have been described in human area 18 (Clarke and Miklossy, 1990; Clarke, 1993). Tracing studies have shown that there are inhomogeneities in the connection patterns within both areas (Burkhalter and Bernardo, 1989; Merigan *et al.,* 1993; Lewis and Olavarria, 1995; Gattass *et al.,* 1997). Others have found subparcellations in the patterns of cytochrome oxidase staining in macaque as well as in human brains (DeYoe and v.Essen, 1985; Livingstone and Hubel, 1987; Krubitzer and Kaas, 1990; Hockfield *et al.,* 1990; Peterhans and von der Heydt, 1993; Wong-Riley *et al.,* 1993; Nakamura *et al.,* 1993; Tootell *et al.,* 1993; Clarke, 1994; Roe and Tso, 1995; Tootell and Taylor, 1995b; Olavarria and v.Essen, 1997; Elston and Rosa, 1998). Considering these data, the final interpretation of intraareal subparcellations would exceed the scope of this cytoarchitectonic study. Therefore, only whole areas 17 and 18 were processed further (3-D reconstruction, transformation to the format of the standard reference brain, and analysis of areas with respect to location and extent).

The areal comparison of mean volumes showed that area 17 was significantly larger than area 18. In the past, volumetric measurements in human brains have been carried out mainly for area 17 (these fit well with our data) and not for 18 (Gerhardt and Kreht, 1933; Rose, 1935; Stephan, 1969; Sauer *et al.,* 1983; Frahm *et al.,* 1984). Therefore, no comparison was carried out between volumes of areas 17 and 18. A study on the visual cortex of the marmoset monkey (Rosa *et al.,* 1997) reported a considerably smaller total surface area of V2 (corresponding roughly to area 18) than of V1 (corresponding to area 17), which is in accordance with data obtained in other animals (Krubitzer and Kaas, 1990; Pessoa *et al.,* 1992). Filimonoff has analyzed both areas in 13 hemispheres of human brains, but he measured surface areas, not volumes. He found a higher proportional size of area 18 than that of area 17 in man (Filimonoff, 1932), but area 17 was relatively larger than area 18 in orangutan and in monkey (Filimonoff, 1933). The composition of his sample, however, was far from optimal—only one female brain was included. More recent studies showed sex differences in volumes (Steinmetz *et al.,* 1995; Amunts *et al.,* 1999a).

Our own analysis of 10 postmortem brains also revealed a considerable intersubject and interhemispheric variability both in the relation of cytoarchitectonic borders to surrounding sulci and gyri and in the

FIG. 5. Surface rendering of the 10 brains and of their cytoarchitectonic areas 17 (red) and 18 (green). View of the occipital lobe. Left hemisphere is left in the images. Note the considerable differences in the extents and shapes of both areas between the cases.

TABLE 2

Ranges and Centers of Gravity (±SD) of Areas 17 and 18 in the Stereotaxic Space ($N = 10$)

		x			*y*			*z*		
Area	Side	From	To	Center of gravity	From	To	Center of gravity	From	To	Center of gravity
17	Right	35	6	20 ± 3	−100	−46	−73 ± 4	−15	21	2 ± 7
	Left	−25	5	−10 ± 4	−104	−50	−77 ± 2	−16	20	3 ± 6
18	Right	41	5	23 ± 2	−99	−43	−71 ± 4	−16	28	6 ± 5
	Left	−30	5	−13 ± 3	−103	−47	−75 ± 3	−16	27	6 ± 5

Note. The coordinates are given according to the atlas system of Talairach and Tournoux (1988).

presence and shape of these landmarks. Filimonoff was one of the first to analyze variability in sulcal patterns quantitatively by calculating coefficients of variation (26 and 25 for areas 17 and 18) on the basis of the surfaces of 17 and 18 (Filimonoff, 1932). Several other studies also have emphasized the variability of this region (Brindley, 1972; Stensaas *et al.,* 1974; v.Essen *et al.,* 1984, 1998; Clark *et al.,* 1996; Dumoulin *et al.,* 1998; Kennedy *et al.,* 1998; Thompson *et al.,* 1998). We have found that the size of area 17 on the exposed surface of the cuneus as well as on the medial and lateral surfaces of the brain was highly variable. This was also true for the calcarine sulcus (Steinmetz *et al.,* 1989; Thompson *et al.,* 1998). Variability can be interpreted as variability into the kind that is not predictable from visual landmarks and the kind that can be related to the sulcal pattern (Rademacher *et al.,* 1993). The variable positions of area 17 on the free surface of the occipital pole and its border to area 18 along the extracalcarine cuneal and lingual planes belong to the first kind. As we have shown in Figs. 5 and 6, there was a large variability in the sulcal pattern. This concerned the shape and continuity of the larger sulci (calcarine, parietooccipital sulcus) and the presence and shape of smaller sulci (Ono *et al.,* 1990; Duvernoy, 1991). In addition to intersubject differences, there were differences between the two hemispheres of one and the same individual in the sulcal pattern and in the relation of areas 17 and 18 to these sulci.

Interhemispheric differences were subjected to further analysis with respect to size and location of both areas. The volumes of both areas did not differ significantly between the hemispheres. Similar findings for area 17 were reported elsewhere (Rademacher *et al.,* 1993). Interhemispheric differences, however, were found in the positions of the areas. Both were located more medially and caudally on the left than on the right. This asymmetry in location of the areas in the postmortem brains mainly reflects a topographical asymmetry of the living human brain. Putative methodological factors (e.g., histological procedure, alignment of brains) which may influence left–right differences in shape obviously play only a minor role. First, in order to minimize the deformation of the brains during histological procedure, their fixation was performed by hanging them up on their vertebral arteries. This is preferable to a fixation of brains which are lying on the bottom of the fixation container and then, due to their own weight, shift to one or the other hemisphere. Although the brains therefore nearly "swim" in the fixative, there is a residual deformation of the occipital poles; i.e., the occipital poles of the fixed brains are pointing outward more than in a brain *in situ.* Thus, compared with stereotaxic data from living human brains (Grady *et al.,* 1996; Hasnain *et al.,* 1998; Goebel *et al.,* 1998), the *x* coordinates (=mediolateral coordinates) of the centers of gravity of both areas were shifted to a more lateral position in our sample. The *y* and *z* coordinates of areas 17 and 18 of the postmortem brains coincide well with those obtained in functional studies of living human brains. However, deformation caused by fixation concerns primarily *both* occipital poles and therefore does not act on asymmetry. Second, the alignment of the postmortem brains to the standard reference brain cannot introduce "artificial" left–right differences because only linear tools, which transform both hemispheres in the same manner, were applied (nonlinear transformation tools were applied only for matching the 3-D reconstructions to the MR sequences). These linear tools reduced intersubject variability in the location and extent of the cytoarchitectonic areas by reducing variability in brain size and position of the postmortem brains. The application of nonlinear fluid transformation would further reduce the variability in brain shape and size, which is influenced, e.g., by sex and handedness, but would not keep left–right differences of the individual postmortem brain. Thus, it

TABLE 3

Coordinates of Areas 17 and 18 by Talairach/Tournoux (Talairach and Tournoux, 1988)

17	Left/right	21	3	—	−100	−65	—	−12	12	—
18	Left/right	37	3	—	−100	−60	—	−16	28	—

Note. Values for sagittal sections are given for both the left and the right hemispheres.

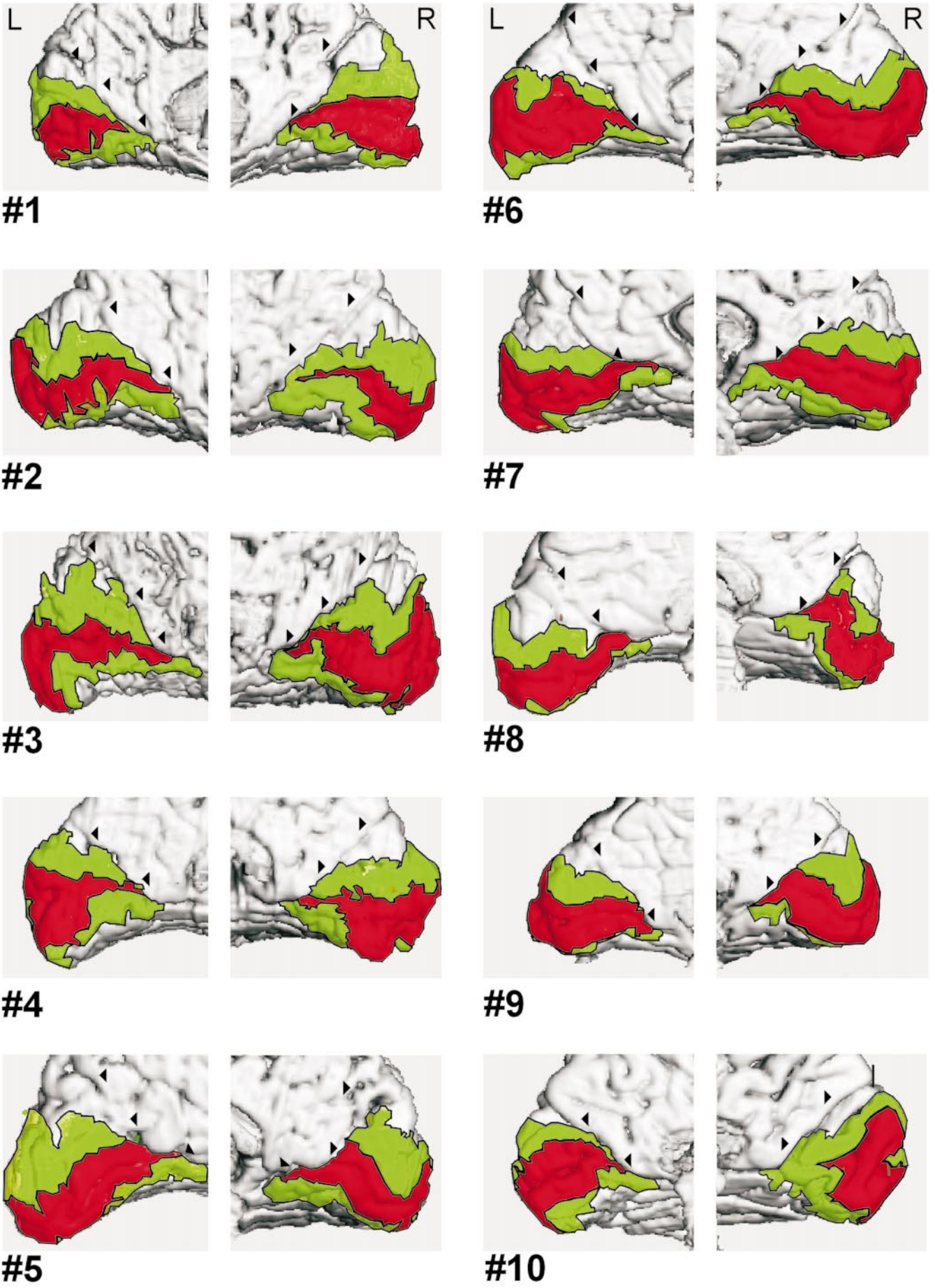

FIG. 6. Surface rendering of left and right hemispheres of the 10 brains and of their cytoarchitectonic areas 17 (red) and 18 (green). View from medial. The cerebellum was removed. L and R, left and right hemispheres, respectively. Arrowheads, parietooccipital sulcus.

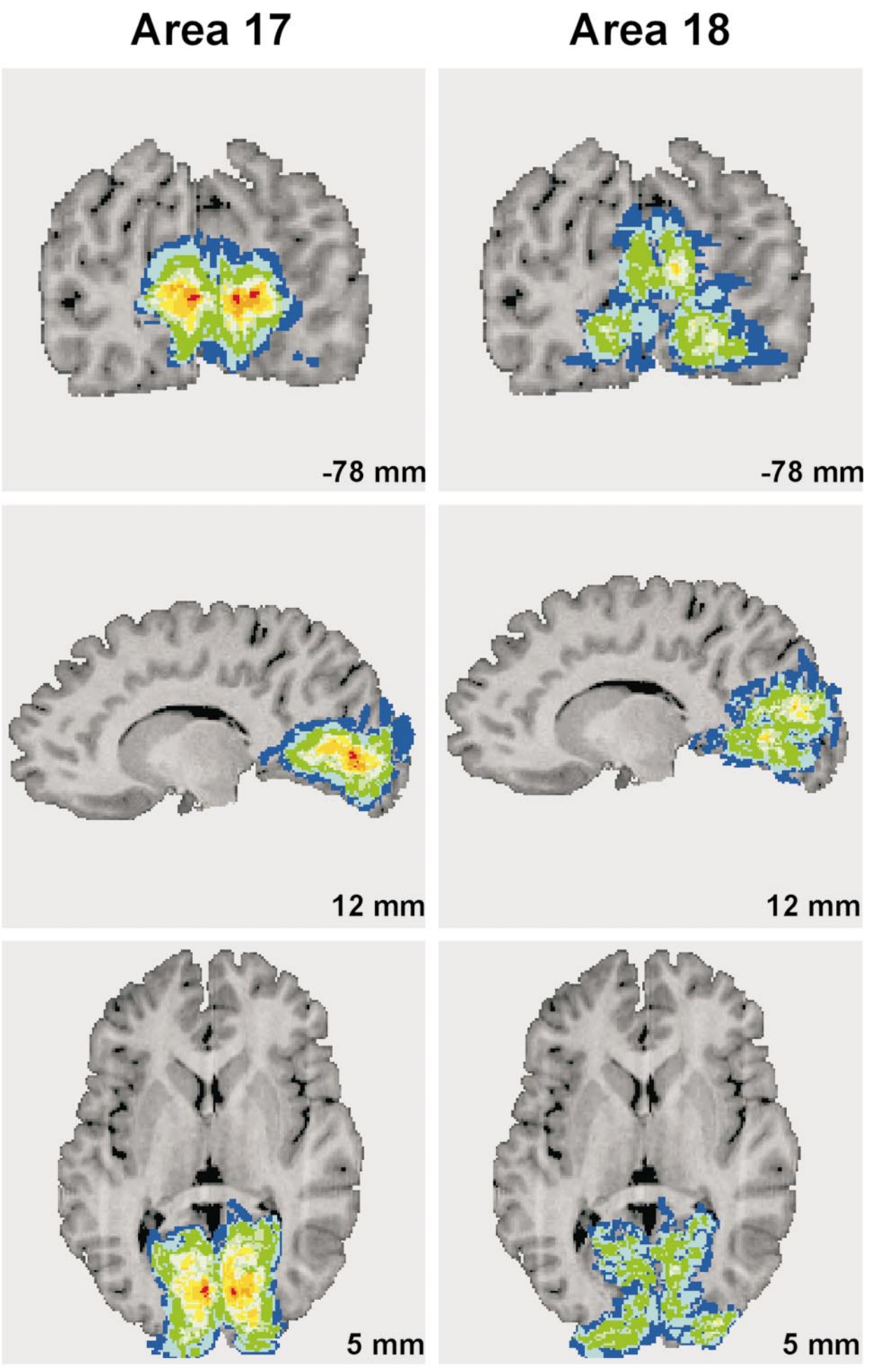
Area 17
Area 18
-78 mm
-78 mm
12 mm
12 mm
5 mm
5 mm
1
10

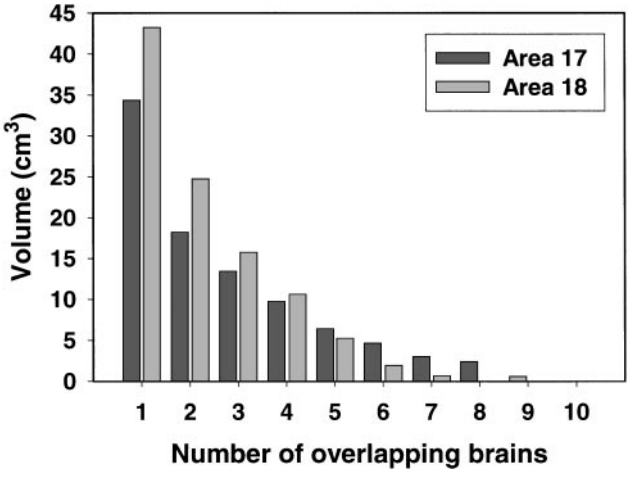

FIG. 8. Quantification of the probability maps. The volumes of areas 17 and 18 are shown relative to the numbers of overlapping brains. The higher the number of overlapping brains the smaller the volumes. The overlap for area 17 is higher than that of area 18. In area 17, even for 10 overlapping brains a volume of 30 mm^3 was found, whereas the corresponding overlap for area 18 is zero.

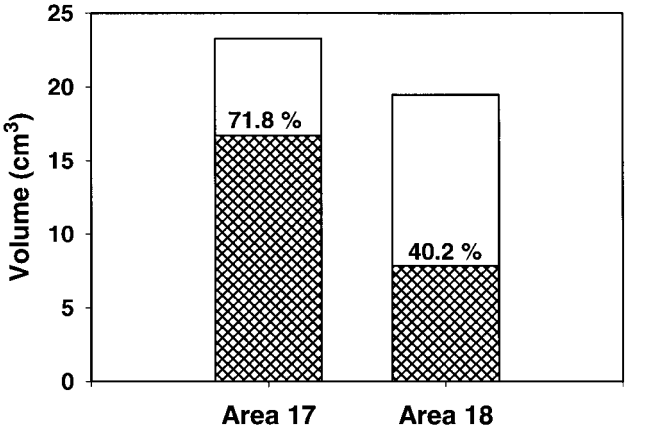

FIG. 9. Mean volumes of area 17 (23.2, SD 3.6 cm^3) and area 18 (19.5 cm^3, SD 3.7) in 10 brains. These volumes are compared with the 50% volumes of each area. The latter correspond to all those voxels in the probability maps which overlap in 5 or more brains. The portion of the 50% volumes in relation to the mean volumes is expressed in %.

removes nonlinear distortion caused by histology, but introduces an asymmetry in shape of the postmortem brain which is determined by the asymmetry of the target brain, i.e., the reference brain (Roland and Zilles, 1994; Zilles *et al.,* 1997; Schormann and Zilles, 1998). Since one of the aims was the analysis of topographical asymmetry, we refrained from applying nonlinear transformation tools for the alignment of the postmortem brains to the reference brain in this study.

Since methodological factors can explain asymmetry only in stereotaxic locations of areas 17 and 18 to a minor degree, it is essentially more important that areas 17 and 18 form a large part of the occipital lobes for which asymmetry has been reported in several observations (LeMay and Kido, 1978; Falk *et al.,* 1991). An MRI analysis of petalia showed especially pronounced petalia in the occipital lobe and on the left side (Zilles *et al.,* 1996). Most of the lateral and medial surfaces of the occipital lobes were protruded more laterally and medially in the left hemisphere than in the right (Zilles *et al.,* 1996). The medial protrusion corresponds to the extent of the visual areas into the right half of the stereotaxic space.

Left–right differences in the positions of areas 17 and 18 are relevant for the anatomical interpretation of clusters of functional activation in imaging studies. The location of these clusters is often attributed to areas according to the stereotaxic atlas of Talairach and Tournoux (1988), which is based on Brodmann's schematic drawing of one left hemisphere. This atlas considers neither left–right nor individual peculiarities, which is especially unfortunate in the case of the occipital lobe where interhemispheric differences in the shape are pronounced. The coordinates for right areas 17 and 18 are grossly underestimated in the Talairach/Tournoux atlas. The remaining coordiantes of this atlas fall within the range of those in our sample, but also tend to underestimate. Functionally defined visual areas also tend to have their centers of mass outside the coordinates given by the Talairach atlas (Hasnain *et al.,* 1998). This is not surprising, since the location of both areas in a single hemisphere cannot adequately represent the range of intersubject and interhemispheric variability.

The variability in the topography of areas 17 and 18 of our study as estimated by SD coincides with the variability of functional areas V1 and V2. As shown recently in a PET study, the standard deviation was 5 mm across eight visual areas tested (Hasnain *et al.,* 1998). A fMRI study analyzing perception of faces found an even higher degree of interindividual variability in the topography of foci than we had found (Clark *et al.,* 1996). SD were 0.7–1.8 cm in the functional study and 0.2–0.7 cm in the present sample.

The importance of sulcal variability as related to variability in size and position will be evaluated when

FIG. 7. Probability maps of areas 17 and 18 in the coronal, sagittal, and horizontal planes. The probability maps are shown in the format of the standard brain. The alignment of the individual brains was performed by using affine transformations (scaling, rotating, shifting). The number of overlapping brains for each voxel is color coded; e.g., yellow means that 7 of 10 brains overlapped in this voxel. Coordinates of the sections according to the Talairach system are at the lower right corners (Talairach and Tournoux, 1988). Note that the variability among the brains is considerable. Left hemisphere is left in the images.

the technique of fluid transformation (instead of only linear, affine ones) for aligning brains has been perfected (Miller *et al.,* 1990; Christensen *et al.,* 1994; Schormann *et al.,* 1996; Drury *et al.,* 1997; Schormann and Zilles, 1998, 1999). This approach can also answer the question whether and to what extent the shape of postmortem brains and of their areas differs from that of living human brains and their functionally defined areas. First results of nonlinear fluid transformations of both areas were used for further analysis of their intersubject variability; they were presented recently (Amunts *et al.,* 1999b).

Summarizing, this study was designed as a basis for an analysis of structural–functional relationships in the human visual system. Such an analysis requires cortical maps with detailed and precise information on the position and extent of cortical areas. Cortical maps should therefore contain spatial and probabilistic information on the position and extent of cortical areas, i.e., the consideration of the individual variability, and they should be based on mapping techniques which allow the delineation of cytoarchitectonic areas by using statistical tools of analysis. Our probability maps of areas 17 and 18 fulfill these criteria: they are based on 10 brains in which the borders of each cytoarchitectonic area were determined by an observer-independent procedure. The information was transferred to the stereotaxic space of the human brain atlas (Roland and Zilles, 1994, 1996). In contrast to the classical anatomical maps which usually contain surface-based information of cytoarchitectonic areas, these data on the location and extent of both areas are in three-dimensional space. Cortical maps of areas 17 and 18 have already been applied in PET studies on the horizontal and vertical meridians (Larsson *et al.,* 1998), on figure–ground segregation in the extrastriate cortex (Larsson *et al.,* 1997), and on processing of color information (Gulyas *et al.,* 1997). Probability maps of areas 17 and 18 are part of the European Computerized Human Brain Database.

ACKNOWLEDGMENTS

The data on areas 17 and 18 are part of the European Computerized Human Brain Database (ECHBD), which was sponsored by BioTech (Roland and Zilles, 1996). The project was also supported by grants of the DFG (SFB 194/A6) and the European Union (BioMed). The authors thank Axel Schleicher, Per Roland, Uli Bürgel, and Kristina Rascher for suggestions and stimulating discussions.

REFERENCES

Aine, C. J., Supek, S. S., George, J. S., Ranken, D., Lewine, J., Sanders, J., Best, E., Tiree, W., Flynn, E. R., and Wood, C. C. 1996. Retinotopic organization of human visual cortex: Departures from the classical model. *Cereb. Cortex* **6:**354–361.

Amunts, K., Jäncke, L., Mohlberg, H., Steinmetz, H., and Zilles, K. 1999a. Interhemispheric asymmetry of the human motor cortex related to handedness and gender. *Neuropsychologia,* in press.

Amunts, K., Klingberg, T., Binkofski, F., Schormann, T., Seitz, R. J., Roland, P. E., and Zilles, K. 1998. Cytoarchitectonic definition of Broca's region and its role in functions different from speech. *NeuroImage* **7:**8.

Amunts, K., Schlaug, G., Schleicher, A., Steinmetz, H., Dabringhaus, A., Roland, P. E., and Zilles, K. 1996. Asymmetry in the human motor cortex and handedness. *NeuroImage* **4:**216–222.

Amunts, K., Schleicher, A., Bürgel, U., Mohlberg, H., Uylings, H. B. M., and Zilles, K. 1999a. Broca's region revisited: Cytoarchitecture and intersubject variability. *J. Comp. Neurol.* **412:**319–341.

Amunts, K., Schmidt-Passos, F., Schleicher, A., and Zilles, K. 1997. Postnatal development of interhemispheric asymmetry in the cytoarchitecture of human area 4. *Anat. Embryol.* **196:**393–402.

Amunts, K., Schormann, T., Mohlberg, H., Malikovic, A., and Zilles, K. 1999b. Location, asymmetry and variability of human areas 17 and 18. *NeuroImage* **9:**861.

Braak, H. 1977. The pigment architecture of the human occipital lobe. *Anat. Embryol.* **150:**229–250.

Brindley, G. S. 1972. The variability of the human striate cortex. *J. Physiol.* **225:**1P–3P.

Brodmann, K. 1903. Beiträge zur histologischen Lokalisation der Grosshirnrinde. II. Der Calcarinustyp. *J. Psychol. Neurol.* **II:**133–159.

Brodmann, K. 1909. *Vergleichende Lokalisationslehre der Großhirnrinde in ihren Prinzipien dargestellt auf Grund des Zellenbaues.* Barth, Leipzig.

Burkhalter, A., and Bernardo, K. L. 1989. Organization of corticocortical connections in human visual cortex. *Proc. Natl. Acad. Sci. USA* **13:**1916–1931.

Christensen, G. E., Rabbitt, R. D., and Miller, M. I. 1994. 3-D brain mapping using deformable neuroanatomy. *Phys. Med. Biol.* **39:**609–618.

Clark, V. P., Keil, K., Maisog, J. M., Courtney, S., Ungerleider, L. G., and Haxby, J. V. 1996. Functional magnetic resonance imaging of human visual cortex during face matching: A comparison with positron emission tomography. *NeuroImage* **4:**1–15.

Clarke, S. 1993. Callosal connections and functional subdivision of the human occipital lobe. In *Functional Organization of the Human Visual Cortex* (B. Gulyas, D. Ottoson, and P. Roland, Eds.), pp. 137–149. Pergamon Press, Oxford.

Clarke, S. 1994. Modular organization of human extrastriate visual cortex: Evidence from cytochrome oxidase pattern in normal and macular degeneration cases. *Eur. J. Neurosci.* **6:**725–736.

Clarke, S., and Miklossy, J. 1990. Occipital cortex in man: Organization of callosal connections, related cyto- and myeloarchitecture, and putative boundaries of functional visual areas. *J. Comp. Neurol.* **298:**188–214.

DeYoe, E. A., Carman, G. J., Bandettini, P., Glickman, S., Wieser, J., Cox, R., Miller, D., and Neitz, J. 1996. Mapping striate and extrastriate visual areas in human cerebral cortex. *Proc. Natl. Acad. Sci. USA* **93:**2382–2386.

DeYoe, E. A., and v.Essen, D. C. 1985. Segregation of efferent connections and receptive field properties in visual area V2 of the macaque. *Nature* **317:**58–61.

Dixon, W. J., Brown, M. B., Engelman, L., Hill, M. A., and Jennrich, R. I. 1988. *BMDP: Statistical Software Manual.* Univ. of California Press, Berkeley.

Drury, H. A., v.Essen, D. C., Snyder, A. Z., Shulman, G. L., Akbudak, E., Ollinger, J. M., Conturo, T. E., Raichle, M., and Corbetta, M. 1997. Warping fMRI activation patterns onto the visible man atlas using fluid deformations of cortical flat maps. *Neurol. Res.* **5:**S421.

Dumoulin, S. O., Bittar, R. G., Kabani, N. J., Baker, C. L., LeGoualher, G., Pike, G. B., and Evans, A. C. 1998. Quantification of the variability of human area v5/MT in relation to the sulcal pattern in

the parieto-temporo-occipital cortex: A new anatomical landmark. *NeuroImage* **7:**S319–S319.

Duvernoy, H. 1991. *The Human Brain. Surface, Three-Dimensional Sectional Anatomy and MRI.* Springer, Vienna/New York.

Elliot Smith, G. 1907. A new topographical survey of the human cerebral cortex, being an account of the distribution of the anatomically distinct cortical areas and their relationship to the cerebral sulci. *J. Anat.* **41:**237–254.

Elston, G. N., and Rosa, M. G. P. 1998. Morphological variation of layer III pyramidal neurons in the occipitotemporal pathway of the macaque monkey visual cortex. *Cereb. Cortex* **8:**278–294.

Engel, S. A., Glover, G. H., and Wandell, B. A. 1997. Retinotopic organization in human visual cortex and the spatial precision of functional MRI. *Cereb. Cortex* **7:**181–192.

Falk, D., Hildeboldt, C., Cheverud, J., Kohn, L. A. P., Figiel, G., and Vannier, M. 1991. Human cortical asymmetries determined with 3D MR technology. *J. Neurosci. Methods* **39:**185–191.

Fellemann, D. J., and v.Essen, D. C. 1991. Distributed hierarchical processing in the primate cerebral cortex. *Cereb. Cortex* **1:**1–47.

Filimonoff, I. N. 1932. Über die Variabilität der Großhirnrindenstruktur. Mitteilung II. Regio occipitalis beim erwachsenen Menschen. *J. Psychol. Neurol.* **45:**65–137.

Filimonoff, I. N. 1933. Über die Variabilität der Großhirnrindenstruktur. Mitteilung III. Regio occipitalis bei den höheren und niederen Affen. *J. Psychol. Neurol.* **44:**1–96.

Flechsig, P. 1927. *Meine Myelogenetische Hirnlehre mit Biographischer Einleitung.* Springer, Berlin.

Frahm, H. D., Stephan, H., and Baron, G. 1984. Comparison of brain structure volumes in Insectivora and primates. V. Area striata (AS). *J. Brain Res.***25:**537–557.

Franca, J. G., do-Nascimento, J. L. M., Picanco-Diniz, C. W., Quaresma, J. A. S., and Silva, A. L. C. 1997. NADPH-diaphorase activity in area 17 of the squirrel monkey visual cortex: Neuropil pattern, cell morphology and laminar distribution. *Braz. J. Med. Biol. Res.* **30:**1093–1105.

Gallyas, F. 1979. Silver staining of myelin by means of physical development. *Neurol. Res.* **1:**203–209.

Gattass, R., Sousa, A. P., Mishkin, M., and Ungerleider, L. G. 1997. Cortical projections of area v2 in the macaque. *Cereb. Cortex* **7:**110–129.

Gerhardt, E., and Kreht, H. 1933. Zur Volumen- und Oberflächengröße der Area striata. *J. Psychol. Neurol.* **45:**220–224.

Geyer, S., Ledberg, A., Schleicher, A., Kinomura, S., Schormann, T., Bürgel, U., Klingberg, T., Larsson, J., Zilles, K., and Roland, P. E. 1996. Two different areas within the primary motor cortex of man. *Nature* **382:**805–807.

Gilbert, A. N., and Wysocki, C. J. 1992. Hand preference and age in United States. *Neuropsychologia* **30:**601–608.

Goebel, R., Khorram-Sefat, D., Muckli, L., Hacker, H., and Singer, W. 1998. The constructive nature of vision: Direct evidence from functional magnetic resonance imaging studies of apparent motion and motion imagery. *Eur. J. Neurosci.* **10:**1563–1573.

Grady, C. L., Horwitz, B., Pietrini, P., Mentis, M. J., Ungerleider, L. G., Rapoport, S. I., and Haxby, J. V. 1996. Effect of task difficulty on cerebral blood flow during perceptual matching of faces. *Human Brain Mapping* **4074:**227–239.

Gulyas, B., Larsson, J., Amunts, K., Zilles, K., and Roland, P. E. 1997. Cortical regions in the human brain systematically participating in the processing and analysis of colour. *NeuroImage* **5:**2. [Abstract]

Gulyas, B., and Roland, P. E. 1994. Processing and analysis of form, color and binocular disparity in the human brain: Functional anatomy by positron emission tomography. *Eur. J. Neurosci.* **6:**725–736.

Hasnain, M. K., Fox, P. T., and Woldorff, M. G. 1998. Intersubject variability of functional areas in the human visual cortex. *Human Brain Mapping* **6:**301–315.

Haxby, J. V., Horrwitz, B., Ungerleider, L. G., Maisog, J. M., Pietrini, P., and Grady, C. L. 1994. The functional organization of human extrastriate cortex: A PET–rCBF study of selective attention to faces and locations. *J. Neurosci.* **14:**6336–6353.

Hockfield, S., Tootell, R. B. H., and Zaremba, S. 1990. Molecular differences among neurons reveal an organization of human visual cortex. *Proc. Natl. Acad. Sci. USA* **87:**3027–3031.

Kaas, J. H. 1989. Why does the brain have so many visual areas? *J. Cognit. Neurosci.* **1:**121–135.

Kaas, J. H. 1993. The organization of visual cortex in primates: Problems, conclusions, and the use of comparative studies understanding the human brain. In *Functional Organization of the Human Visual Cortex* (B. Gulyas, D. Ottoson, and P. E. Roland, Eds.), pp. 1–12. Pergamon Press, Oxford.

Kaas, J. H. 1995. Progress and puzzles. *Curr. Biol.* **5:**1126–1128.

Kaas, J. H., and Krubitzer, L. A. 1991. The organization of extrastriate visual cortex. In *Neuroanatomy of the Visual Pathways and Their Development* (B. Dreher and S. R. Robinson, Eds.), pp. 303–323. Macmillan, Houndsmills, UK.

Kennedy, D. N., Lange, N., Makris, N., Bates, J., Meyer, J., and Caviness, V. J. 1998. Gyri of the human neocortex: An MRI-based analysis of volume and variance. *Cereb. Cortex* **8:**372–384.

Kleinschmidt, A., Lee, B. B., Requard, M., and Frahm, J. 1996. Functional mapping of color processing by magnetic resonsnce imaging of responses to selective P- and M-pathway stimulation. *Exp. Brain Res.* **110:**279–288.

Krubitzer, L. A., and Kaas, J. H. 1990. Cortical connections of MT in four species of primates: Areal, modular and retinotopic pattern. *Visual Neurosci.* **5:**165–204.

Larsson, J., Amunts, K., Gulyas, B., Malikovic, A., Zilles, K., and Roland, P. E. 1998. Functional and anatomical delineation of human visual areas: A multiple-criteria approach. *NeuroImage* **7:**305.

Larsson, J., Gulyas, B., Amunts, K., Zilles, K., and Roland, P. E. 1997. Figure–ground segregation activates human extrastriate visual cortex. *NeuroImage* **5:**167.

LeMay, M., and Kido, D. K. 1978. Asymmetries of the cerebral hemispheres on computed tomograms. *J. Comput. Assisted Tomogr.* **2:**471–476.

Leuba, G., and Garey, L. R. 1989. Comparison of neuronal and glial numerical density in primary and secondary visual cortex of man. *Exp. Brain Res.* **77:**31–38.

Lewis, J. W., and Olavarria, J. F. 1995. Two rules for callosal connectivity in striate cortex of the rat. *J. Comp. Neurol.* **361:**119–137.

Livingstone, M. S., and Hubel, D. H. 1987. Connections between layer 4B of area 17 and the thick cytochrome oxidase stripes of area 18 in the squirrel monkey. *J. Neurosci.* **7:**3371–3377.

Lueck, C. J., Zeki, S., Friston, K. J., Deiber, M. P., Cope, P., Cunningham, V. J., Lammertsma, A. A., Kennard, C., and Frackowiak, R. S. J. 1989. The colour centre in the cerebral cortex of man. *Nature* **340:**386–389.

Lungwitz, W. 1937. Zur myeloarchitektonischen Untergliederung der menschlichen Area praeoccipitalis (Area 19 Brodmann). *J. Psychol. Neurol.* **47:**607–638.

Malach, R., Reppas, J. B., Benson, R. R., Kwong, K. K., Jiang, H., Kennedy, W. A., Ledden, P. J., Brady, T. J., Rosen, B. R., and Tootell, R. B. H. 1995. Object-related activity revealed by functional magnetic resonance imaging in human occipital cortex. *Proc. Natl. Acad. Sci. USA* **92:**8135–8139.

Mazziotta, J. C., Toga, A. W., Evans, A. C., Fox, P. T., and Lancaster,

J. L. 1995. A probabilistic atlas of the human brain: Theory and rationale for its development. *NeuroImage* **2:**89–101.

Merigan, W. H., Nealey, T. A., and Maunsell, J. R. 1993. Visual effects of lesions of cortical area v2 in macacques. *J. Neurosci.* **13:**3180–3191.

Merker, B. 1983. Silver staining of cell bodies by means of physical development. *J. Neurosci.* **9:**235–241.

Miller, M. I., Christensen, G. E., Amit, Y., and Grenander, U. 1990. Mathematical textbook of deformable neuroanatomies. *Proc. Natl. Acad. Sci. USA* **90:**11944–11948.

Nakamura, H., Gattass, R., Desimone, R., and Ungerleider, L. G. 1993. The modular organization of projections from areas V1 and V2 to areas V4 and TEO in macaques. *J. Neurosci.* **13:**3681–3691.

Olavarria, J. F., and v.Essen, D. C. 1997. The global pattern of cytochrome oxidase stripes in visual area V2 of the macaque monkey. *Cereb. Cortex* **7:**395–404.

Ono, M., Kubik, S., and Abernathey, C. D. 1990. *Atlas of the Cerebral Sulci*. Thieme, Stuttgart/New York.

Pearson, K. 1936. Method of moments and method of maximum likehood. *Biometrika* **28:**34–59.

Pessoa, V. F., Abrahao, J. C. H., Pacheco, R. A., Pereira, L. C. M., Magalhaes-Castro, B., and Saraiva, P. E. S. 1992. Relative sizes of cortical visual areas in marmosets: Functional and phylogenetic implications. *Exp. Brain Res.* **88:**459–462.

Peterhans, E., and von der Heydt, R. 1993. Functional organization of area V2 in the alert monkey. *Eur. J. Neurosci.* **5:**509–524.

Portin, K., Salenius, S., Salmelin, R., and Hari, R. 1998. Activation of the human occipital and parietal cortex by pattern and luminance stimuli: Neuromagnetic measurements. *Cereb. Cortex* **8:**253–260.

Rademacher, J., Caviness, J., Steinmetz, H., and Galaburda, A. M. 1993. Topographical variation of the human primary cortices: Implications for neuroimaging, brain mapping, and neurobiology. *Cereb. Cortex* **3:**313–329.

Riegele, L. 1931. Die Cytoarchitektonik der Felder der Broca'schen Region. *J. Psychol. Neurol.* **42:**496–514.

Roe, A. W., and Tso, D. Y. 1995. Visual topography in primate v2: Multiple representation across functional stripes. *J. Neurosci.* **15:**3689–3715.

Roland, P. E., and Zilles, K. 1994. Brain atlases—A new research tool. *Trends Neurosci.* **17:**458–467.

Roland, P. E., and Zilles, K. 1996. The developing European computerized human brain database for all imaging modalities. *NeuroImage* **4:**S39–S47.

Roland, P. E., and Zilles, K. 1998. Structural divisions and functional fields in the human cerebral cortex. *Brain Res. Rev.* **26:**87–105.

Rosa, M. G. P., Fritsches, K. A., and Elston, G. N. 1997. The second visual area in the marmoset monkey: Visuotopic organization, magnification factors, architectonical boundaries, and modularity. *J. Comp. Neurol.* **387:**547–567.

Rose, M. 1935. Cytoarchitektonik und Myeloarchitektonik der Großhirnrinde. In: *Handbuch der Neurologie* (O. Bumke and O. Foerster, Eds.), pp. 588–778. Springer, Berlin.

Sanides, F. 1963. Die Architektonik des menschlichen Stirnhirns und die Prinzipien seiner Entwicklung. *Fortschritte Med.* **81:**831–838.

Sanides, F., and Vitzhum, H. G. 1965a. Die Grenzerscheinungen am Rande der menschlichen Sehrinde. *Dtsch. Z. Nervenheilk.* **187:**708–719.

Sanides, F., and Vitzhum, H. G. 1965b. Zur Architektonik der menschlichen Sehrinde und den Prinzipien ihrer Entwicklung. *Dtsch. Z. Nervenheilk.* **187:**680–707.

Sarkisov, S. A., Filimonoff, I. N., and Preobrashenskaya, N. S. 1949. *Cytoarchitecture of the Human Cortex Cerebri.* Medgiz, Moscow. [In Russian]

Sauer, B., Kammradt, G., Krauthausen, I., Kretschmann, H.-J., Lange, H. W., and Wingert, F. 1983. Qualitative and quantitative development of the visual cortex in man. *J. Comp. Neurol.* **214:**441–450.

Schleicher, A., Amunts, K., Geyer, S., Kowalski, T., and Zilles, K. 1998. An observer-independent cytoarchitectonic mapping of the human cortex using a stereological approach. *Acta Stereol.* **17:**75–82.

Schleicher, A., Amunts, K., Geyer, S., Morosan, P., and Zilles, K. 1999. Observer-independent method for microstructural parcellation of cerebral cortex: A quantitative approach to cytoarchitectonics. *NeuroImage* **9:**165–177.

Schleicher, A., and Zilles, K. 1990. A quantitative approach to cytoarchitectonics: Analysis of structural inhomogeneities in nervous tissue using an image analyzer. *J. Microsc.* **157:**367–381.

Schormann, T., Dabringhaus, A., and Zilles, K. 1995. Statistics of deformations in histology and improved alignment with MRI. *IEEE Trans. Med. Imag.* **14:**25–35.

Schormann, T., Henn, S., and Zilles, K. 1996. A new approach to fast elastic alignment with application to human brains. *Lect. Notes Comp. Sci.* **1131:**437–442.

Schormann, T., v.Matthey, M., Dabringhaus, A., and Zilles, K. 1993. Alignment of 3-D brain data sets originating from MR and histology. *Bioimaging* **1:**119–128.

Schormann, T., and Zilles, K. 1997. Limitations of the principle axes theory. *IEEE Trans. Med. Imag.* **16:**942–947.

Schormann, T., and Zilles, K. 1998. Three-dimensional linear and nonlinear transformations: An integration of light microscopical and MRI data. *Human Brain Mapping* **6:**339–347.

Schormann, T., Dabringhaus, A., and Zilles, K. 1997. Extension of the principal axis theory for the determination of altine transformations. Proceeding of the DAGH: Informatik Aktuell., pp. 384–391. Berlin, Germany. Springer–Verlag.

Sereno, M. I., Dale, A. M., Reppas, J. B., Kwong, K. K., Belliveau, J. W., Brady, T. I., Rosen, B. R., and Tootell, R. B. H. 1995. Borders of multiple visual areas in humans revealed by functional magnetic resonance imaging. *Science* **268:**889–893.

Shipp, S., Watson, J. D. G., Frackowiak, R. S. J., and Zeki, S. 1995. Retinotopic maps in human prestriate visual cortex: The demarcation of areas V2 and V3. *NeuroImage* **2:**125–132.

Steinmetz, H., Fürst, G., and Meyer, B. U. 1989. Craniocerebral topography within the international 10–20 system. *Electroencephalogr. Clin. Neurophysiol.* **72:**495–506.

Steinmetz, H., Rademacher, J., Jäncke, L., Huan, Y., Thron, A., and Zilles, K. 1990. Total surface of temporoparietal intrasylvian cortex: Diverging left–right asymmetries. *Brain Lang.* **39:**357–372.

Steinmetz, H., Staiger, J. F., Schlaug, G., Huang, Y., and Jäncke, L. 1995. Corpus callosum and brain volume in women and men. *NeuroReport* **6:**1002–1004.

Stensaas, S. S., Eddington, D. K., and Dobelle, W. H. 1974. The topography and variability of the primary visual cortex in man. *J. Neurosurg.* **40:**747–757.

Stephan, H. 1969. Quantitative investigations on visual structures in primate brains. In *Proc. 2nd Int. Congr. Primatol., Atlanta, Georgia, 1968,* pp. 34–42. Karger, Basel.

Stepniewska, I., and Kaas, J. H. 1996. Topographic patterns of V2 cortical connections in macaque monkeys. *J. Comp. Neurol.* **371:**129–152.

Talairach, J., and Tournoux, P. 1988. *Coplanar Stereotaxic Atlas of the Human Brain.* Thieme, Stuttgart.

Thompson, P. M., Moussai, J., Zohoori, S., Goldkorn, A., Khan, A. A., Mega, M. S., Small, G. W., Cummings, J. L., and Toga, A. W. 1998. Cortical variability and asymmetry in normal aging and Alzheimer's disease. *Cereb. Cortex* **8:**492–509.

Tootell, R. B. H., Born, R. T., and Ash-Bernal, R. 1993. Cortical organization in visual cortex in non-human primates and man. In *Functional Organization of the Human Visual Cortex* (B. Gulyas, D. Ottoson, and P. E. Roland, Eds.), pp. 59–74. Pergamon Press, Oxford.

Tootell, R. B. H., Mendola, J. D., Hadjikhani, N. K., Ledden, P. J., Liu, A. K., Reppas, J. B., Sereno, M. I., and Dale, A. M. 1997. Functional analysis of V3A and related areas in human visual cortex. *J. Neurosci.* **17:**7060–7078.

Tootell, R. B. H., Reppas, J. B., Kwong, K. K., Malach, R., Born, R. T., Brady, T. J., Rosen, B. R., and Belliveau, J. W. 1995a. Functional analysis of human MT and related visual cortical areas using magnetic resonance imaging. *J. Neurosci.* **15:**3215–3230.

Tootell, R. B. H., and Taylor, J. B. 1995b. Anatomical evidence for MT and additional cortical visual areas in humans. *Cereb. Cortex* **5:**39–55.

Ungerleider, L. G. 1995. Functional brain imaging studies of cortical mechanisms for memory. *Science* **270:**769–775.

v.Economo, C., and Koskinas, G. N. 1925. *Die Cytoarchitektonik der Hirnrinde des Erwachsenen Menschen.* Springer, Berlin.

v.Essen, D. C., Drury, H. A., and Lewis, J. W. 1998. Comparison among cortical partitioning schemas within and across species using surface-based atlases. *NeuroImage* **7:**S741.

v.Essen, D. C., Fellemann, D. J., DeYoe, E., and Knierim, J. J. 1993. Probing the primate visual cortex: Pathways and perspectives. In *Functional Organization of the Human Visual Cortex* (B. Gulyas, D. Ottoson, and P. E. Roland, Eds.), pp. 29–42. Pergamon Press, Oxford.

v.Essen, D. C., Newsome, W. T., and Maunsell, H. R. 1984. The visual field representation in the striate cortex of the macacque monkey: Asymmetries, anisotropies, and individual variability. *Visual Res.* **24:**429–448.

Vogt, C., and Vogt, O. 1919. Allgemeinere Ergebnisse unserer Hirnforschung. *J. Psychol. Neurol.* **25:**292–398.

Vogt, M. 1929. Über fokale Besonderheiten der Area occipitalis. *J. Psychol. Neurol.* **39:**4–6.

Watson, J. D. G., Frackowiak, R. S. J., and Zeki, S. 1993. Functional separation of colour and motion centres in human visual cortex. In *Functional Organization of the Human Visual Cortex* (B. Gulyas, D. Ottoson, and P. E. Roland, Eds.), pp. 317–328. Pergamon Press, Oxford.

Wong-Riley, M. T., Hevner, R. F., Cutlan, R., Earnest, M., Egan, R., Frost, J., and Nguyen, T. 1993. Cytochrome oxidase in the human visual cortex: Distribution in the developing and the adult brain. *Visual Neurosci.* **10:**41–58.

Wree, A., Schleicher, A., and Zilles, K. 1982. Estimation of volume fractions in nervous tissue with an image analyzer. *J. Neurosci. Methods* **6:**29–43.

Zeki, S. 1993. *A Vision of the Brain.* Blackwell, Oxford.

Zilles, K., Armstrong, E., Schlaug, G., and Schleicher, A. 1986. Quantitative cytoarchitectonics of the posterior cingulate cortex in primates. *J. Comp. Neurol.* **253:**514–524.

Zilles, K., and Clarke, S. 1997. Architecture, connectivity and transmitter receptors of human extrastriate visual cortex. Comparison with non-human primates. In *Cerebral Cortex* (Rockland *et al.,* Ed.), Vol. 12, pp. 673–742. Plenum, New York.

Zilles, K., Dabringhaus, A., Geyer, S., Amunts, K., Qü, M., Schleicher, A., Gilissen, E., Schlaug, G., Seitz, R., and Steinmetz, H. 1996. Structural asymmetries in the human forebrain and the forebrain of non-human primates and rats. *Neurosci. Behav. Rev.* **20:**593–605.

Zilles, K., Schlaug, G., Matelli, M., Luppino, G., Schleicher, A., Qü, M., Dabringhaus, A., Seitz, R., and Roland, P. E. 1995. Mapping of human and macaque sensorimotor areas by integrating architectonic, transmitter receptor, MRI and PET data. *J. Anat.* **187:**515–537.

Zilles, K., and Schleicher, A. 1993. Cyto- and myeloarchitecture of human visual cortex and the periodical GABA-A receptor distribution. In *Functional Organization of the Human Visual Cortex* (B. Gulyas, D. Ottoson, and P. Roland, Eds.), pp. 111–120. Pergamon Press, Oxford.

Zilles, K., Schleicher, A., Langemann, C., Amunts, K., Morosan, P., Palomero-Gallagher, N., Schormann, T., Mohlberg, H., Bürgel, U., Steinmetz, H., Schlaug, G., and Roland, P. E. 1997. A quantitative analysis of sulci in the human cerebral cortex: Development, regional heterogeneity, gender difference, asymmetry, intersubject variability and cortical architecture. *Human Brain Mapping* **5:**218–221.

Zilles, K., Werners, R., Büsching, U., and Schleicher, A. 1986. Ontogenesis of the laminar structures in area 17 and 18 of the human visual cortex. A quantitative study. *Anat. Embryol.* **174:**129–144.